

# Photochemistry of Products of the Aqueous Reaction of Methylglyoxal with Ammonium Sulfate

Paige K. Aiona,<sup>†</sup> Hyun Ji Lee,<sup>†</sup> Renee Leslie,<sup>†</sup> Peng Lin,<sup>‡</sup> Alexander Laskin,<sup>‡</sup> Julia Laskin,<sup>‡</sup> and Sergey A. Nizkorodov<sup>\*,†</sup>

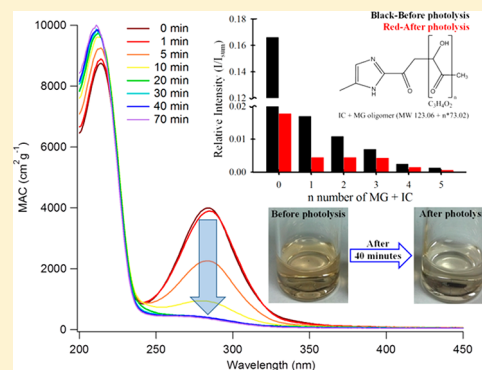
<sup>†</sup>Department of Chemistry, University of California, Irvine, California 92697, United States

<sup>‡</sup>Department of Chemistry, Purdue University, West Lafayette, Indiana 47907, United States

## Supporting Information

**ABSTRACT:** Aqueous reactions of methylglyoxal (MG) and glyoxal with ammonium sulfate (AS) produce light-absorbing compounds (chromophores) and may serve as a source of atmospheric secondary “brown carbon” (BrC). The molecular composition of these chromophores is ambiguous, and their transformation due to exposure to solar UV radiation is not well understood. We examined the molecular composition, mass absorption coefficients, and fluorescence spectra of BrC samples produced by the evaporation of aqueous MG/AS solutions. Chromatograms of BrC produced by evaporation were different from those of BrC produced by slow MG/AS reaction in water, highlighting the substantial sensitivity of BrC to its formation conditions. The BrC samples were characterized before and after their exposure to broadband (270–390 nm) UV radiation. Irradiation led to rapid photobleaching, a decrease in the characteristic 280 nm absorption band, a complete loss of fluorescence, and a dramatic change in molecular composition. By comparing the composition before and after the irradiation, we identified several structural motifs that may contribute to the light-absorbing properties of MG/AS BrC. For example, a family of oligomers built from an imidazole carbonyl and repetitive MG units was prominent in the initial sample and decreased in abundance after photolysis. More complex oligomers containing both imidazole and pyrrole rings in their structures also appeared to contribute to the pool of BrC chromophores. The selective reduction of carbonyl functional groups by sodium borohydride diminished the absorption but had little effect on the fluorescence of MG/AS BrC samples, suggesting that absorption in this system is dominated by individual chromophores as opposed to supramolecular charge-transfer complexes. Due to the efficient photolysis of the BrC chromophores, this MG/AS BrC system has limited impact on the direct radiative forcing of climate but may have an effect on atmospheric photochemistry in aerosol particles.

**KEYWORDS:** brown carbon aerosol, aqueous photolysis, photobleaching, photodegradation, mass absorption coefficient, excitation–emission matrix, charge-transfer complexes



## 1. INTRODUCTION

Methylglyoxal (MG) is produced by gas-phase oxidation of many anthropogenic and biogenic volatile organic compounds (VOC) including benzene, toluene, ethylbenzene, xylenes, C<sub>3</sub>–C<sub>5</sub> alkanes, isoprene, acetone, monoterpenes, and methylbutenol (see Fu et al.<sup>1</sup> and references therein). Biofuel and biomass burning are also known to directly emit MG into the atmosphere. As a result, MG is commonly observed in urban, rural, and remote environments, with an estimated global annual production of about 140 Tg/year.<sup>1</sup>

Several laboratory and field studies have shown that the uptake of MG (and of the structurally related glyoxal, G) by wet aerosols and cloud droplets and its subsequent aging proceed through several competing aqueous-phase chemical processes, including (1) aqueous oxidation, which in the case of MG produces water-soluble glyoxylic, pyruvic, and oxalic acids; (2) formation of *gem*-diols followed by oligomerization into high molecular weight products; and (3) ammonium-catalyzed

condensation and formation of imidazole compounds.<sup>1–3</sup> Some of these processes result in the formation of light-absorbing compounds that may affect the optical properties of secondary organic aerosols (SOA) formed in the aqueous phase.<sup>1,2,4,5</sup> Specifically, the products of MG reacting with ammonium sulfate (AS) have an absorption band at 280 nm, as well as a weak absorption tail that extends into the visible range. The presence of this absorption tail makes MG + AS and G + AS reactions a potential source of “brown carbon” (BrC).<sup>2</sup>

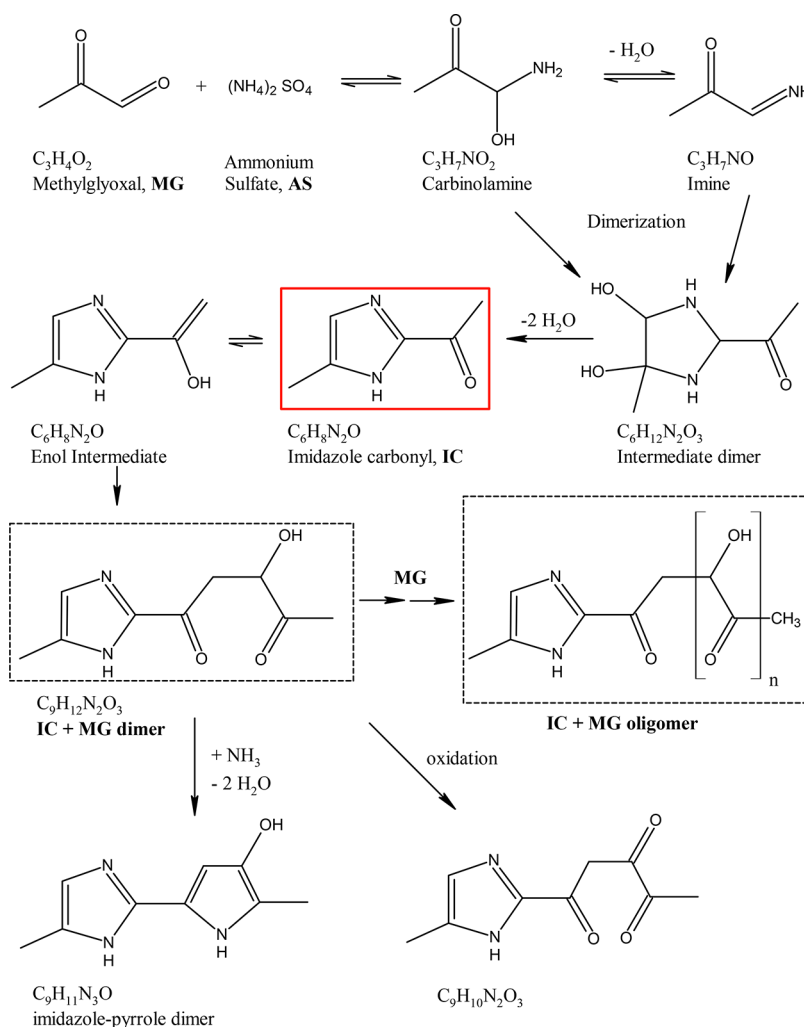
A number of recent studies have characterized the products formed in aqueous reactions of MG and G (see ref 2 for a comprehensive review of the recent literature). For example, De Hann et al. performed structural analysis of the products of

Received: July 4, 2017

Revised: August 28, 2017

Accepted: September 1, 2017

Published: September 1, 2017

Scheme 1. MG + AS Reactions Leading to the Formation of the Imidazole Carbonyl and Its Oligomers<sup>a</sup>

<sup>a</sup>Adapted with permission from De Haan et al. IC is the well-known product of the MG + AS reaction; the dashed boxes indicate possible structures of the oligomers observed in this work. The bottom part of the scheme shows possible reactions of IC + MG oligomers including pyrrole ring formation and oxidation.

MG reactions with AS, amino acids, and methyl amine and observed nitrogen-containing oligomers of imidazole.<sup>6,7</sup> Scheme 1 adopted from De Haan et al. shows some of the processes relevant to this work.<sup>7</sup> Sareen et al. used chemical ionization mass spectrometry to study the reaction of MG with AS and observed aldol condensation products, high-molecular-weight oligomers, and sulfur- and nitrogen-containing compounds.<sup>8</sup> Maxut et al. measured molar extinction coefficients of several expected products of G and AS.<sup>9</sup> The imidazole carbonyl (IC) shown in Scheme 1 likely makes the dominant contribution to the 280 nm absorption peak; however, the molecular identities of the absorbers in the red tail of the spectrum remain ambiguous.<sup>9–11</sup>

Although numerous studies have examined MG/AS reactions under dark conditions,<sup>2</sup> much less is known about the photochemical properties of the resulting BrC products (referred to as MG/AS BrC for the rest of the article). Sareen et al. examined the stability of MG/AS BrC with respect to UV photolysis and oxidative aging by  $O_3$  and/or OH radicals and concluded that photolysis is the primary daytime sink of this type of BrC in the atmosphere, with a characteristic lifetime on the order of minutes.<sup>12</sup> This short lifetime suggests that MG/

AS BrC accumulating in aqueous reactions overnight is quickly removed upon sunrise and is not likely to have a strong effect on direct radiative forcing.<sup>12–14</sup> Similarly, Zhao et al. reported that MG/AS BrC exhibits rapid photochemical bleaching in the aqueous phase by a combination of direct photolysis and OH oxidation. They estimated that the atmospheric lifetime of MG/AS BrC ranges from minutes to a few hours.<sup>15</sup>

Concentrated aqueous solutions of MG and AS develop brown color on a time scale of hours to days,<sup>8</sup> but this process can be dramatically accelerated by evaporating the solution. For example, Lee et al. demonstrated that evaporation of aerosolized G/AS aqueous solutions produces BrC orders of magnitude faster than observed in bulk solutions.<sup>16</sup> In our previous work, we used high-performance liquid chromatography paired with a photodiode array detector and high-resolution mass spectrometry (HPLC-PDA-HRMS) to characterize MG/AS BrC formed via slow aqueous reaction.<sup>17</sup> In this work, we characterized the molecular composition, absorption spectra, and fluorescence spectra of MG/AS BrC accelerated by evaporation of MG solutions containing AS. The changes in molecular composition of MG/AS BrC, before and after UV photolysis, were analyzed by high-resolution mass spectrometry

(HRMS). We found that aqueous photolysis of MG/AS BrC not only decreases its absorption and fluorescence intensity but also results in a significant change in molecular composition. We explored the response of selected BrC species to photolysis using HPLC-PDA-HRMS. We carried out a reduction of MG/AS BrC compounds by sodium borohydride ( $\text{NaBH}_4$ ), which is commonly used to selectively reduce carbonyl groups into alcohols and disrupt charge-transfer (CT) complexes formed by the interaction between donor ( $-\text{OH}$ ) and acceptor ( $=\text{O}$ ) groups.<sup>18,19</sup> The absorption peak at 280 nm was eliminated by  $\text{NaBH}_4$  reduction, but the fluorescence was mostly unaffected, implying that CT complexes do not strongly contribute to light-absorption properties in the MG/AS system. Additionally, this reduction eliminated all but one chromophore seen in the MG/AS BrC chromatogram. Our results support the conclusion that MG/AS BrC is a highly dynamic system that is quite unstable under solar irradiation, as previously concluded by Sareen et al.<sup>12</sup> and Zhao et al.<sup>15</sup> Although this BrC system will have a marginal impact on the direct radiative forcing of climate, it may have a profound effect on atmospheric photochemistry occurring in fog droplets and wet aerosols.

## 2. EXPERIMENTAL METHODS

### 2.1. Methylglyoxal and Ammonium Sulfate Mixtures.

A 0.1 M stock solution of MG was prepared by diluting a commercial MG solution in deionized water (Sigma-Aldrich, 40% in  $\text{H}_2\text{O}$ ). A 0.1 M stock solution of AS was prepared by dissolving 1.32 g of AS (Fisher Scientific,  $\geq 99\%$ ) in 100 mL of deionized water. The two stock solutions were mixed in a 1:1 ratio by volume, resulting in a 0.05 M concentration of each reactant in the initial solution (corresponding to 3.6 g/L MG and 6.6 g/L AS). The browning of this mixture occurs fairly slowly at room temperature, over the course of several days. In order to speed up the browning process,<sup>7,16,20</sup> the mixed sample was immediately evaporated in a scintillation vial attached to a Buchi Rotavapor R-215 at 30 °C until all solvent was removed. Whereas the full evaporation process took  $\sim 20$  min, the residue acquired brown color only at the end of the evaporation process, in the last minute, when most of the water was evaporated from the sample. Evaporation could have been done faster at a higher evaporation temperature, but we did not want to deviate too much from typical ambient temperatures. The brown residue formed during the evaporation was then redissolved in the same amount of deionized water as the initial volume of the mixed MG and AS solutions. This redissolution process may lead to a partial reversal of the reactions occurring upon evaporation, but the brown color of the final solution suggests that at least some of the BrC compounds produced in evaporation are stable with respect to hydrolysis. It is also possible that some MG was lost during the evaporation step, but we had no easy way of quantifying this loss. The products formed during the evaporation differ from those formed in the slower browning process, as implied by the difference in the HPLC-PDA-HRMS data for samples obtained by these two methods. The evaporation-driven products are likely to be more environmentally relevant because they can be produced faster, after a single cloud processing cycle.

### 2.2. Optical Properties and Photolysis of MG/AS BrC.

Following evaporation and redissolution, each MG/AS BrC sample was diluted to achieve an absorbance less than one at 280 nm in order to avoid deviations from Beer's law. The resulting concentrations of organics in the diluted solutions (0.5–0.8 g/L) listed in Table 1 are based on the mass of MG

Table 1. Summary of Photolysis Experiments<sup>a</sup>

sample no.	concentration of BrC (g/L)	absorbance decay rate ( $\text{s}^{-1}$ )	QY
1	0.60	$1.5 \times 10^{-3}$	0.46
2	0.60	$2.3 \times 10^{-3}$	0.59
3	0.80	$2.2 \times 10^{-3}$	0.98
4	0.54	$1.2 \times 10^{-3}$	0.33
average $\pm$ SD			$0.59 \pm 0.28$

<sup>a</sup>For each MG/AS sample, the estimated BrC mass concentration (taken to be equal to the mass concentration MG would have had after redissolution and dilution if it was not reactive), the measured 280 nm absorbance decay rate, and the effective quantum yield (QY) value calculated from eq 2 are listed. The average QY and its standard deviation (SD) are listed, as well.

used in the initial reaction mixture and the total volume used to reach an absorbance less than one at 280 nm. This calculation neglects the possible MG mass loss by evaporation and mass gain due to aqueous chemistry. A dual-beam spectrophotometer (Shimadzu UV-2450) was used to record the UV/vis absorption spectra of the diluted samples in the 200–700 nm range. Three-dimensional excitation–emission matrix (EEM) spectra were acquired with a Hitachi F-4500 fluorescence instrument.<sup>16</sup> The excitation wavelength spanned the 200–500 nm range in 5 nm steps, and the emission was recorded over the 300–600 nm range in 2 nm increments. Deionized water served as the background for the absorption and EEM measurements. For all samples, back-to-back absorption and fluorescence measurements were conducted before and after photolysis.

The procedure for photolysis of the MG/AS BrC samples was similar to that described by Epstein et al.<sup>21</sup> Briefly, the sample in a standard 1.0 cm cuvette was placed in a temperature-controlled cuvette holder. The cuvette was irradiated from the top with broadband UV radiation delivered from a xenon arc lamp housing (Newport model 6256) through a 0.95 cm liquid light guide. Before entering the light guide, the UV radiation was reflected with a 90° dichroic mirror and filtered with a U-330 band-pass filter (Edmund optics #46-438). The height of the irradiated samples was kept consistent by using a constant volume of 2.5 mL in the cuvette. No change in solution volume was visible throughout the photolysis experiments. A small magnetic stir bar mixed the sample during photolysis. For the MG/AS BrC samples, the absorbance at 280 nm was continuously measured through the side of the cuvette to determine the effective photolysis rate, listed in Table 1. This experiment was repeated four times with four independently prepared samples. In addition, a complete absorption spectrum was periodically recorded (the stir bar was stopped during these measurements).

The spectral flux density of the UV radiation was determined by photolyzing a 0.1 M solution of azoxybenzene (Fisher Scientific, 98%) in ethanol in the presence of 0.1 M potassium hydroxide, as described by Lee et al.<sup>22</sup> Azoxybenzene is a convenient actinometer because its photolysis quantum yield ( $\text{QY}_{\text{azo}} \sim 0.020$ ) is not strongly dependent on temperature and concentration.<sup>23</sup> The actinometer measurements were conducted prior to and after photolysis of the MG/AS BrC samples. The radiation flux density was determined from the increase in absorption of the azoxybenzene photoisomer (molar absorption coefficient of  $7600 \text{ L mol}^{-1} \text{ cm}^{-1}$  at 458 nm) as a function of irradiation time.<sup>22</sup> Most of the photolyzing radiation

fell within the 270–390 nm range with a peak flux of  $\sim 1.5 \times 10^{14}$  photon  $\text{cm}^{-2} \text{s}^{-1} \text{nm}^{-1}$  occurring near 320 nm (Figure S1). Based on the measured flux, the effective quantum yield (QY) of MG/AS BrC photolysis was calculated, as described in the Supporting Information. For direct comparison, similar analysis was done for the photolysis of brown compounds produced by the reaction of limonene ozonolysis SOA with ammonia (aged LIM/O<sub>3</sub> SOA). Details of the aged LIM/O<sub>3</sub> SOA production and measurements were described in Lee et al.<sup>22</sup>

**2.3. Electrospray Ionization High-Resolution Mass Spectrometry (ESI-HRMS).** A separate set of aged and photolyzed MG/AS BrC samples was analyzed using a high-resolution ( $m/\Delta m \sim 10^5$  at  $m/z$  450) linear-ion-trap Orbitrap (Thermo Corp.) electrospray ionization mass spectrometer (ESI-HRMS) operated in positive ion mode. The dissolved analytes were detected as sodiated  $[M + \text{Na}]^+$  and protonated  $[M + \text{H}]^+$  species. A calibration mixture of caffeine MRFA and Ultramark 1621 (LTQ ESI Positive Ion Calibration Solution, Thermo Scientific, Inc.) was used to calibrate the  $m/z$  axis at the beginning and end of each day. In each set of the experiments, a MG/AS BrC sample was prepared, as described in section 2.1. Half of the sample was photolyzed for 40 min, while the other half was kept in the dark as a control. Photolysis led to a complete loss of the brown color of the sample. After the photolysis, both the control and photolyzed samples were diluted with acetonitrile (Aldrich, HPLC grade) in a 1:1 ratio to improve the ESI source stability. A blank sample, corresponding to a 1:1 mixture of acetonitrile and water, was also prepared. The control, photolyzed, and blank samples were then analyzed using ESI-HRMS. This type of photolysis experiment was repeated twice for reproducibility.

The data analysis protocol was similar to that used by Lee et al.<sup>22</sup> Briefly, internal calibration of the  $m/z$  axis, with respect to the expected MG/AS BrC products, resulted in a mass accuracy of better than  $\pm 0.0005$  Da in the  $m/z$  range of 100–800. Peaks that appeared in the blank sample and peaks corresponding to <sup>13</sup>C isotopes were filtered out. Only peaks that reproducibly appeared in both sets of independent measurements were retained. The peaks were assigned molecular formulas with the atomic restrictions of  $\text{C}_{2-42}\text{H}_{2-80}\text{O}_{0-35}\text{N}_{0-4}\text{Na}_{0-1}^+$  and a tolerance of 0.00075  $m/z$  while constraining the H/C and O/C ratios to 0–1.0 and 0.3–2.0, respectively, and only permitting closed-shell ions (no ion radicals). For ambiguous assignments, the preference was to assign peaks to a formula with fewer N atoms. This preference is based on the prevalence of compounds containing low N atom numbers for the unambiguously assigned peaks. For clarity, all of the formulas discussed in this paper correspond to neutral analytes (with H<sup>+</sup> or Na<sup>+</sup> removed from the ion formula).

**2.4. Selective Reduction of Carbonyls by NaBH<sub>4</sub>.** Sharpless and Blough reported that NaBH<sub>4</sub> selectively reduces carbonyl groups that act as acceptors in the CT process.<sup>19</sup> To test for the potential contribution of the CT complexes to the measured absorption and fluorescence, a new set of MG/AS BrC samples was prepared as described in section 2.1, diluted to achieve a 280 nm absorbance of less than one, and reacted with solid NaBH<sub>4</sub>.<sup>18</sup> Prior to the NaBH<sub>4</sub> addition, absorbance, fluorescence, and pH of the diluted MG/AS BrC solutions were measured. At this point, the pH of the MG/AS solution was around 4. After the addition of  $\sim 0.6$  mg of NaBH<sub>4</sub> to 3.5 mL of the diluted sample, the absorption spectrum was continuously measured every 5 min for about 20 h. We observed an increase, as opposed to the anticipated decrease, in the absorbance. Once

the increase in the absorbance slowed down, about  $\sim 4.7$  mg of additional NaBH<sub>4</sub> was added and the absorption spectrum was continuously measured again for 2–4 h. This second addition of NaBH<sub>4</sub> led to the anticipated decrease in absorbance. After taking the last absorption spectrum, the pH of the samples was around 9. In order to match the starting pH of the MG/AS BrC solution before the NaBH<sub>4</sub> addition, the pH was adjusted from 9 back to 4 using dropwise addition of 1 M HCl. Once corrected, the absorbance and fluorescence were measured. The study was repeated twice, both under O<sub>2</sub> and N<sub>2</sub> purging conditions. While the reduction was taking place, an identical control sample without NaBH<sub>4</sub> was left in the dark for comparison. Absorbance and fluorescence spectra of this sample were taken at the beginning and end of the study.

**2.5. HPLC-PDA-HRMS.** Both the photolysis and NaBH<sub>4</sub> reduction samples were analyzed using a HPLC-PDA-HRMS platform, along with a dark control sample. Analysis was done using procedures identical to those used by Lin et al.<sup>17</sup> The HPLC pump and PDA detector were part of the Surveyor Plus system, and the high-resolution mass spectrometer was a LTQ-Orbitrap with a standard IonMAX electrospray ionization (ESI) source (all modules are from Thermo Electron, Inc.). The separation was done with a SM-C18 column (Imtakt Scherzo SM-C18, SM035, 130 Å pore size, 3 μm particles, 150 × 3.0 mm). The column was operated at a CH<sub>3</sub>CN/H<sub>2</sub>O binary mobile phase with a 200 μL min<sup>-1</sup> flow rate using the following elution protocol: a 3 min hold at 10% of CH<sub>3</sub>CN, a 43 min linear gradient to 90% CH<sub>3</sub>CN, a 7 min hold at this level, a 1 min return to 10% CH<sub>3</sub>CN, and another hold until the total scan time of 80 min. No desalting processing was done before the separation. The PDA detector was used to take UV/vis spectra from 250 to 700 nm, whereas the ESI settings were as follows: positive ionization mode, +4 kV spray potential, 35 units of sheath gas flow, 10 units of auxiliary gas flow, and 8 units of sweep gas flow. Data were analyzed using Xcalibur software (Thermo Scientific), and formulas were assigned with a molecular formula calculator (<http://magnet.fsu.edu/~midas/>).

### 3. RESULTS AND DISCUSSION

**3.1. Mass Absorption Coefficients of MG/AS BrC.** The initial solution before evaporation contained 3.6 g/L MG and 6.6 g/L AS. These values are considerably higher than concentrations of organics and ammonium sulfate in cloud/fogwater but lower than the concentrations expected for aerosol liquid water.<sup>24</sup> Table 1 summarizes the effective BrC concentrations (0.5–0.8 g/L) of the solutions obtained after the evaporation, redissolution, and dilution and subsequently used for the photolysis experiments. The effective BrC mass concentration in these solutions was assumed to be equal to what the mass concentration of MG would have been if it was unreactive toward AS. This is an approximation because we do not know how much MG was lost during the evaporation of the MG/AS samples and how much MG reacted in the browning process. Furthermore, we do not account for NH<sub>3</sub> and water that may have been incorporated into the organic products during the evaporative aging.

Figure 1a shows the bulk mass absorption coefficient (MAC) of MG/AS BrC as a function of wavelength calculated using eq 1 from the measured base-10 absorbance,  $A_{10}$ , mass concentration,  $C_{\text{mass}}$ , and path length,  $b = 1$  cm.<sup>25</sup>

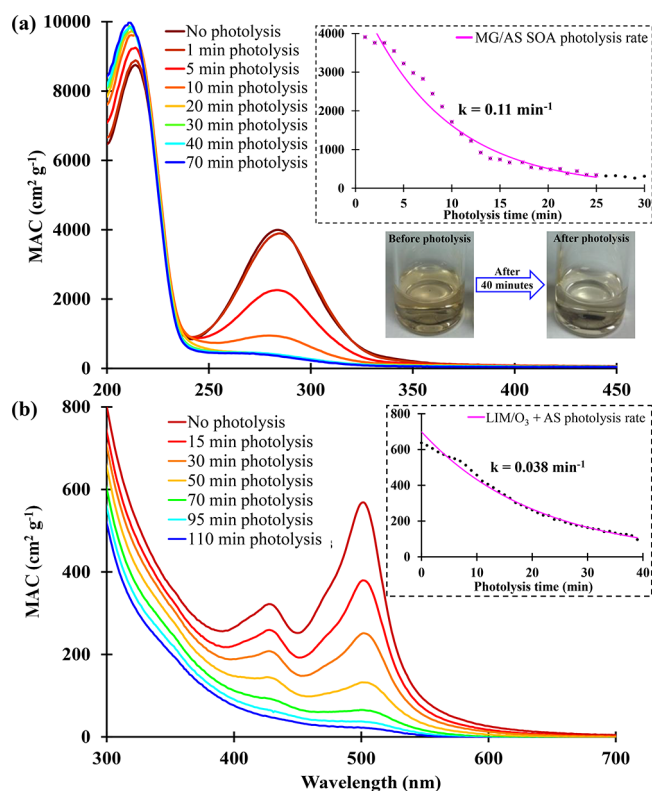


**Figure 1.** Wavelength-dependent mass absorption coefficients (MAC, calculated from eq 1) of (a) MG/AS BrC and (b) aged LIM/O<sub>3</sub> SOA taken at different photolysis times. The right corner of each panel shows the time dependence of MAC for MG/AS BrC at 280 nm and for aged LIM/O<sub>3</sub> SOA at 500 nm. The photo illustrates the change in the MG/AS BrC sample color from brown to colorless during photolysis.

$$\text{MAC}(\lambda) = \frac{A_{10}^{\text{solution}}(\lambda) \times \ln(10)}{b \times C_{\text{mass}}} \quad (1)$$

The MAC values shown in Figure 1a represent an average of the data for the four samples listed in Table 1, using the MG concentration as  $C_{\text{mass}}$  in eq 1. Because of the uncertainty in the mass concentrations of BrC, the MAC values should be regarded as order-of-magnitude estimates. Nevertheless, the maximum MAC value of  $0.4 \text{ m}^2 \text{ g}^{-1}$  at 280 nm is quite high and comparable to MAC for biomass burning organic aerosols ( $0.2\text{--}3 \text{ m}^2 \text{ g}^{-1}$ ).<sup>2</sup> The MAC values for the aged LIM/O<sub>3</sub> SOA shown in Figure 1b for comparison are an order of magnitude lower. However, unlike the MG/AS reaction products, which only absorb in the near-UV range, the aged LIM/O<sub>3</sub> SOA absorbs throughout the visible range where it can have a much stronger effect on direct radiative forcing.

**3.2. Effective Quantum Yield of Photolysis.** The inset of Figure 1a shows the effect of photolysis on MAC at 280 nm, that is, at the peak of the BrC absorption spectrum. MAC was efficiently decreased by photolysis, and the decay rate in MAC was approximately exponential with a first-order rate constant of  $0.11 \text{ min}^{-1}$ . After  $\sim 30$  min of photolysis, the solution became colorless, as shown in the inset of Figure 1a, and the MAC at visible wavelengths ( $\lambda = 400\text{--}700 \text{ nm}$ ) dropped below the limit of detection. The corresponding MAC values of aged LIM/O<sub>3</sub> SOA and the effect of photolysis on that system are shown in Figure 1b for comparison. The loss of the characteristic

absorption band at 500 nm occurred at a slower rate of  $0.038 \text{ min}^{-1}$  under comparable experimental conditions.

Quantitative interpretation of these measurements is complicated because of the large number of individual absorbers in the BrC solution. One possible approach is to expand the usual definition of photolysis quantum yield for a single absorber to a complex mixture of absorbing compounds (eq 2).

$$\text{QY} = \frac{\text{rate}_{\text{photolysis}}}{\text{rate}_{\text{absorption}}} \quad (2)$$

In this case, multiple compounds absorb radiation, with some of them breaking or isomerizing and others disposing of the excitation energy without undergoing a reaction. The rate of absorption by the mixture can be calculated without making any approximations by measuring the known spectral flux density and wavelength-dependent absorbance, as described in Lee et al.<sup>22</sup> The rate of photolysis can be obtained from the measured absorbance decay rates (e.g., Figure 1a) using an assumption that all molecules in the mixture have the same average formula and identical photophysical properties. In this approach, the application of eq 2 to our data generates an *effective photolysis quantum yield*. This QY shows what fraction of the absorbed photons would result in photolysis if all the BrC molecules were the same.

Table 1 lists all of the calculated absorbance decay rates used in the QY calculation for MG/AS BrC samples using eq 2. Further details of the calculations are provided in the Supporting Information. The inferred QY values ranged from 0.33 to 0.98. The low level of reproducibility suggests that the effective QY may be sensitive to the distribution of BrC chromophores. The average QY for the four measurements was  $0.59 \pm 0.28$ , which means that a large fraction of photons that are absorbed lead to the loss of the MG/AS BrC chromophores. The high QY value implies a very short lifetime of the electronically excited state, suggesting a direct photolysis process that is occurring in a singlet excited state. We carried out similar analysis for the photobleaching of the aged LIM/O<sub>3</sub> SOA solution shown in Figure 1b. The effective QY for the aged LIM/O<sub>3</sub> SOA was  $\sim 0.26$ , which is also quite high. Therefore, we expect that both types of BrC will be photobleached promptly by sunlight, lowering their potential impact on climate.

**3.3. Photolysis Effect on Fluorescence of Aged MG/AS.** In order to determine the effect of photolysis on fluorescence and the fluorescence quantum yield for the MG/AS BrC samples, EEM spectra were generated. The EEM in Figure 2a shows that MG/AS BrC is weakly fluorescent. The EEM observed in this work is qualitatively similar to the EEM reported in refs 26 and 27, with the peak occurring at  $\lambda_{\text{ex}} \sim 330 \text{ nm}$  and  $\lambda_{\text{em}} \sim 400 \text{ nm}$ . The fluorescence quantum yield ( $\text{QY}_{\text{F}}$ ) was analyzed as described in Lee et al.<sup>16</sup> Compared to previously studied BrC model systems, such as aged LIM/O<sub>3</sub> SOA with  $\text{QY}_{\text{F}}$  of 0.002 and naphthalene/OH SOA with  $\text{QY}_{\text{F}}$  of 0.003, the  $\text{QY}_{\text{F}}$  for MG/AS BrC was an order of magnitude higher, at 0.02.<sup>22</sup> This value is comparable to the  $\text{QY}_{\text{F}}$  of  $\sim 0.02$  in ambient samples reported by Phillips et al.<sup>18</sup> The fluorescence disappeared almost completely after 40 min of photolysis. This behavior is similar to that in aged LIM/O<sub>3</sub> SOA but opposite to SOA produced by photo-oxidation of naphthalene, for which the fluorescence intensity increased with photolysis.<sup>22</sup> Our results confirm that fluorescence of secondary

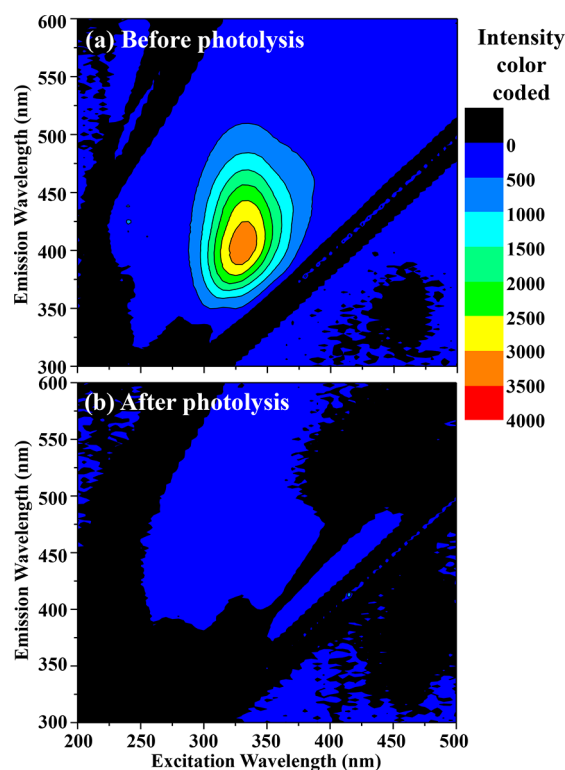


**Figure 2.** EEMs recorded (a) before and (b) after 40 min of photolysis of a MG/AS BrC sample. The relative fluorescence intensity is indicated with the color bar.

BrC is highly dependent on the structures of BrC chromophores.<sup>8,15,18,22</sup>

**3.4. Molecular Composition of MG/AS BrC.** Figure 3 compares direct infusion ESI mass spectra acquired before and after photolysis of aqueous MG/AS BrC samples, and Table S1 provides a list of all the reproducibly observed formulas. The

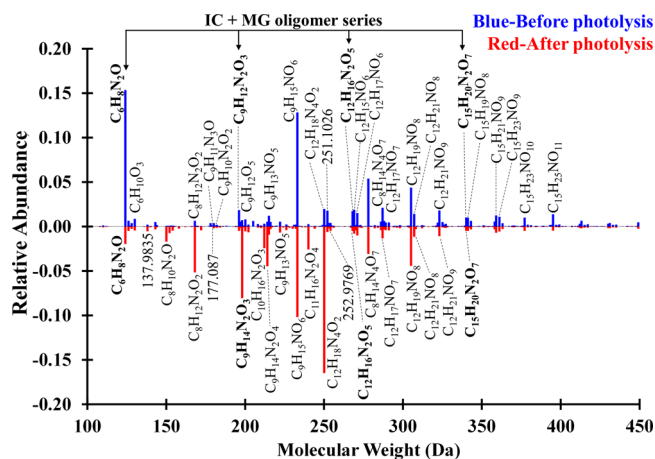


**Figure 3.** Reconstructed mass spectra of assigned peaks in the MG/AS BrC samples before (positive signal) and after (negative signal) photolysis. The peak abundances are normalized with respect to the total ion current, with the normalized abundances of all the peaks adding up to 1. Abundant peaks are labeled with the corresponding neutral formulas. The removal of higher molecular weight compounds during photolysis is clearly evident from the spectra. The IC + MG oligomers (Scheme 1) are highlighted in bold and shown with an arrow on the “before photolysis” side.

mass spectrum of the unphotolyzed sample is qualitatively consistent with the ESI mass spectrum of products of reactions of MG and AS in evaporating droplets reported by De Haan et al.<sup>7</sup> The most abundant peak in Figure 3 corresponds to the imidazole carbonyl (IC,  $C_6H_8N_2O$ ), observed as a protonated ion at  $m/z$  125.0709, which is also one of the major peaks in the mass spectrum in Figure 1 of De Haan et al. The second most abundant peak in the unphotolyzed sample is  $C_9H_{15}NO_6$ , appearing as a protonated ion at  $m/z$  234.0972, which is the largest peak in the De Haan et al. mass spectrum. Other prominent peaks of protonated ions in Figure 3 include  $C_8H_{14}N_4O_7$  at  $m/z$  279.0935,  $C_{12}H_{19}NO_8$  at  $m/z$  306.1183, and  $C_{12}H_{21}NO_9$  at  $m/z$  324.1289. A series of IC + MG oligomers, formed by the reaction of enol forms of IC with  $n$  MG molecules, were also observed. Scheme 1, adopted from De Haan et al.,<sup>7</sup> presents a possible mechanism for the formation of these IC + MG oligomers. Scheme S1 shows possible structures for larger oligomers not included in Scheme 1.

In addition to the imidazole-based compounds containing two nitrogen atoms and imidazole-based dimers containing four nitrogen atoms, compounds containing three nitrogen atoms were also observed. Such compounds can be readily produced by replacing any of the carbonyl groups in the primary products by an imine group. The imine–carbonyl equilibrium usually strongly favors the carbonyl, but the imines may be stabilized by intramolecular reactions leading to stable aromatic rings. For example, the IC + MG oligomers have multiple carbonyl groups in 1,4 arrangement, which can form stable pyrrole-based ring structures in  $NH_3$ -mediated reactions.<sup>10</sup> Scheme 1 shows a plausible pathway for IC + MG dimer  $C_9H_{12}N_2O_3$  to undergo such a reaction. A formula corresponding to the expected  $C_9H_{11}N_3O$  product was found in the ESI-HRMS spectrum and is listed in Table S1. Finally, the distribution of observed formulas implies that oxidation of the hydroxyl groups to carbonyl groups was occurring in solution. For example, the IC + MG dimer  $C_9H_{12}N_2O_3$  can be oxidized to  $C_9H_{10}N_2O_3$ , as shown in Scheme 1.

The 40 min of photolysis, during which MG/AS BrC lost its brown color, resulted in a substantial change in the mass spectrum. Table S1 provides a list of the observed formulas and indicates whether peaks decreased or increased in relative abundance after photolysis. Some peaks were completely removed during photolysis, and several new peaks appeared in the photolyzed sample. The peak intensities of the IC + MG oligomers decreased greatly with photolysis, as shown in Figure 4. Nitrogen-containing heterocyclic oligomers have been identified as the plausible light-absorbing compounds in the MG/AS mixture;<sup>17</sup> the loss of the IC + MG oligomers occurring in parallel with photobleaching suggests that they may contribute to the visible light absorption of the mixture. All of the imidazole–pyrrole complex oligomers (compounds with three nitrogen atoms) also decreased in peak abundance with photolysis, suggesting that they may contribute to the light-absorbing properties of MG/AS BrC.

Despite the large effect of the photolysis on the molecular composition, the average properties of MG/AS BrC did not change significantly. For example, there was a very small net decrease in the average DBE (double bond equivalent, Figure S2), almost no change in the average atomic ratios (Table S2), and almost no change in the N atom distribution between the BrC compounds (Table S3). The average molecular formula of MG/AS BrC remained essentially the same after photolysis:

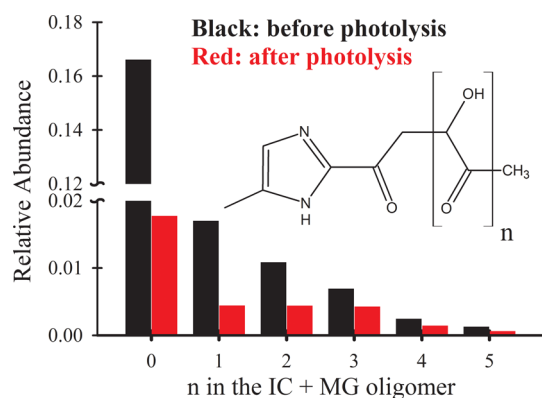
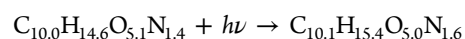


**Figure 4.** Effect of photolysis on the relative intensity of the IC + MG oligomers that are shown in Scheme 1, for  $n = 0$ –5.



The formulas for the peaks that appeared during photolysis were not qualitatively different (in terms of the average size and average atomic ratios) from the formulas of compounds that disappeared during photolysis. These observations suggest that the average properties, such as the  $\langle \text{O}/\text{C} \rangle$  and  $\langle \text{N}/\text{C} \rangle$  ratios, are not good indicators of the extent of photolysis-driven molecular changes in the MG/AS BrC system. This conclusion is similar to that reached in our recent study of aqueous photolysis of SOA generated from different precursors<sup>28</sup> and in the photolysis of  $\alpha$ -pinene SOA particles.<sup>29</sup>

**3.5. NaBH<sub>4</sub> Reduction of Carbonyls.** Adding a small amount of NaBH<sub>4</sub> ( $\sim 0.6$  mg) to MG/AS BrC resulted in a

slight red shift in the absorption peak, as shown in Figure 5a; then, over about 20 h, the absorbance continuously increased. This was not expected because the selective reduction of carbonyl groups to alcohols by NaBH<sub>4</sub> is supposed to eliminate CT complexes, decreasing the absorbance at longer wavelengths.<sup>18</sup> Once this increase in the absorbance slowed down, an excess amount of NaBH<sub>4</sub> (4.7 mg) was added; this led to the anticipated decrease in absorbance after about 3 h (Figure 5a). These observations suggest that the effect of NaBH<sub>4</sub> on the MG/AS BrC is not limited to selective reduction of carbonyl groups; more complex chemistry must be occurring. Although the exact mechanism is unclear, the eventual decrease in the absorbance suggests that the carbonyl groups in MG/AS BrC are essential parts of the chromophores (e.g., IC shown in Scheme 1 is known to have a high extinction coefficient). The results of these experiments were the same under both O<sub>2</sub> and N<sub>2</sub> purging conditions, suggesting that oxygen does not play a significant role in the borohydride reduction chemistry.

We note that the increase in the pH of the MG/AS solution upon addition of NaBH<sub>4</sub> may have side effects on the reaction mechanism, complicating the interpretation of the results. The pH of the solution increased from 4 to about 9 as a result of adding the excess amount of NaBH<sub>4</sub>. Readjusting the pH to match the pH of the initial MG/AS BrC solution after evaporation and dilution further decreased the absorbance (Figure 5a). The change in pH from the addition of NaBH<sub>4</sub> may shut down the acid-catalyzed and/or enable base-catalyzed aldol condensation reactions. The aldol condensation mechanism is known to be important for the formation of light-absorbing products in the MG/AS system, as demonstrated by

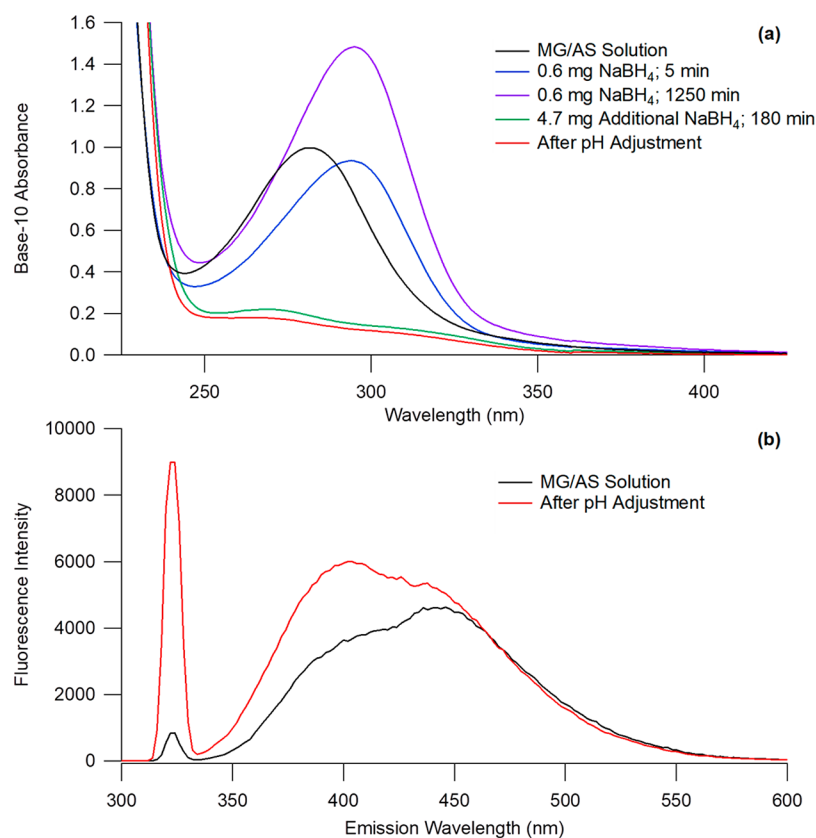


**Figure 5.** Effect of the MG/AS BrC + NaBH<sub>4</sub> reduction in an O<sub>2</sub>-containing solution on the (a) absorption spectrum and (b) fluorescence spectrum excited at 325 nm. Similar results were obtained in a duplicate study under conditions of N<sub>2</sub> bubbling through the solution.

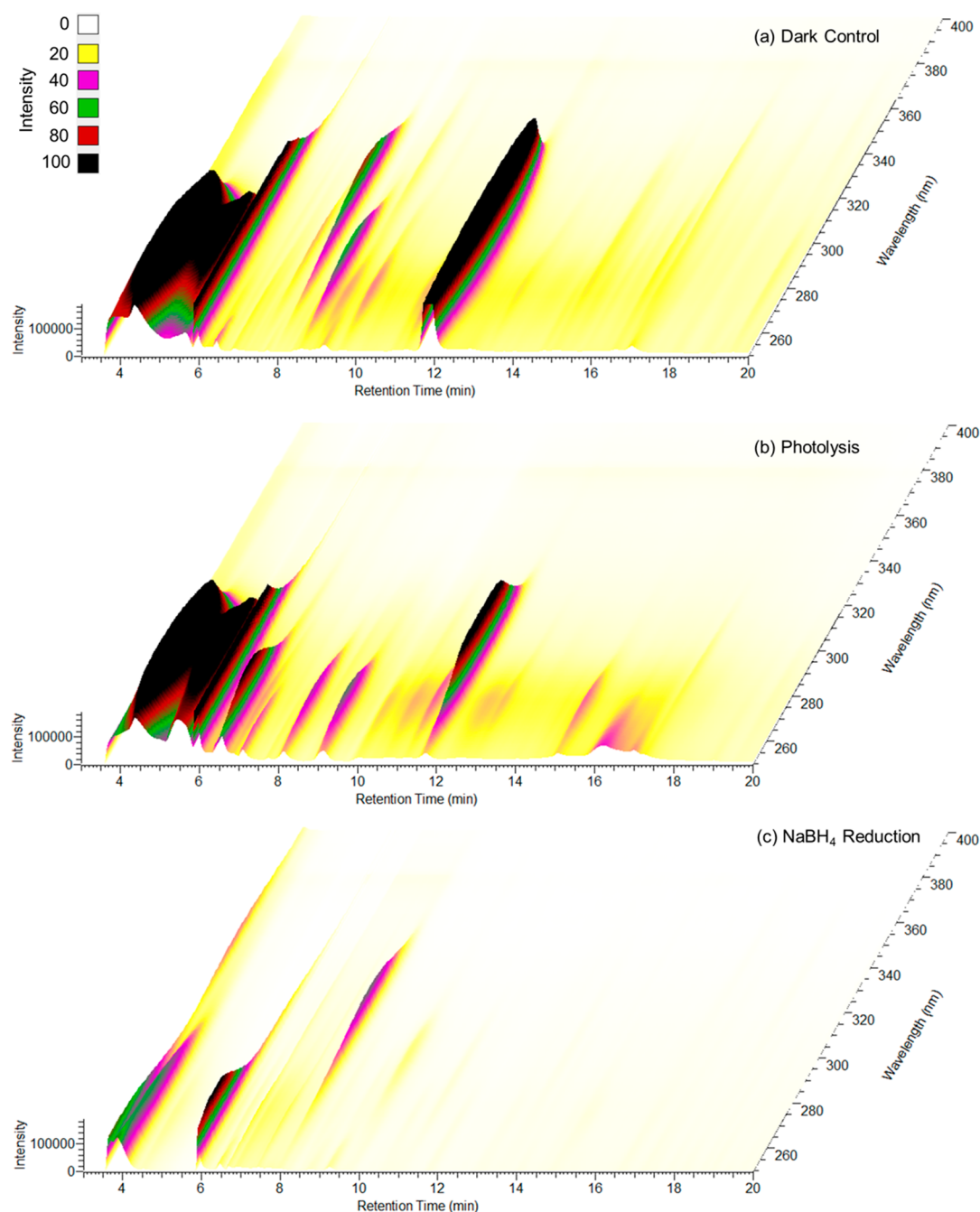


**Figure 6.** HPLC-PDA chromatograms for the MG/AS (a) dark control, (b) photolyzed sample, and (c) NaBH<sub>4</sub> reduction sample after excess NaBH<sub>4</sub> was added. The PDA absorbance is indicated by the color (darker color = higher absorbance).

Sareen et al.<sup>8</sup> Therefore, the reduction of the carbonyls by NaBH<sub>4</sub> may have to compete with pH-induced changes in the aldol formation equilibria.

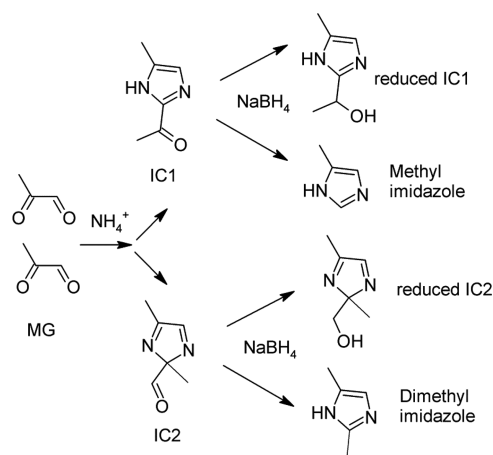
While the absorption at 280 nm decreased with the addition of the excess NaBH<sub>4</sub>, the fluorescence intensity increased slightly (Figure 5b). In contrast, both the absorption and fluorescence decreased during photolysis (Figures 1 and 2). This difference in behavior suggests that the primary chromophores responsible for the 280 nm absorption, which are removed by both methods, are different from the fluorophores, which decrease with photolysis and increase with NaBH<sub>4</sub> reduction. In other words, the molecular subsets of the chromophores and fluorophores in MG/AS BrC do not fully overlap.

**3.6. HPLC-PDA-HRMS.** Figure 6 shows PDA chromatograms for the dark control (a), photolysis (b), and NaBH<sub>4</sub> reduction (c) MG/AS BrC samples. The wavelength range is limited to 250–400 nm in Figure 6 in order to emphasize the chromophores contributing to the near-UV range. For each peak in the PDA chromatograms, we used the approach of Lin et al.<sup>17</sup> to find molecular formulas that give well-defined peaks in the selected ion chromatogram (SIC) at the same time that the absorbing species are eluting in the PDA chromatogram (after accounting for a known time delay between the PDA and ESI-MS detectors). Whereas this approach worked for a few of the PDA peaks, we could not definitively assign formulas to all of them because of the dominating abundance of ions that did not correspond to any of the chromophores and eluted over a

broad range of elution times. For example, the mass spectra for retention times below 6 min were very complex and included peaks from various ionic complexes built from ammonium, sulfate, bisulfate, and organic ions. Furthermore, most of the PDA peaks correlated to more than one candidate ion, and conversely, SICs for many candidate ions had peaks at more than one retention time.

The largest PDA peak occurred at 12 min in the chromatogram for the dark control sample in Figure 6a. It correlated well with the  $m/z$  125.0709 SIC and was assigned to the protonated IC. This  $m/z$  was also the largest peak in the direct infusion ESI mass spectrum of the unphotolyzed MG/AS BrC sample shown in Figure 3. The 12 min UV/vis absorption spectrum acquired by the PDA had a broad peak near 290 nm, in qualitative agreement with the absorption spectra reported previously<sup>9–11</sup> for the related IC formed from glyoxal. The PDA chromatogram had additional peaks at shorter retention times in the  $m/z$  125.0709 SIC (Figure S3), suggesting possible structural isomers of IC or in-source fragmentation. Scheme 2

**Scheme 2. Two Possible Structural Isomers of the Imidazole Carbonyl and Processes Involved in Their Reaction with NaBH<sub>4</sub>**



shows that the MG + AS reaction may potentially produce two structural isomers of IC. The isomer IC2 should have its carbonyl group converted into a *gem*-diol in an aqueous solution, and it is expected to be more polar and elute at earlier times. The isomer IC1 should be more stable than IC2 because of the aromatic stabilization of IC1 and more stable with respect to hydration. Therefore, IC1 must be the chromophoric species eluting at 12 min. Larger compounds, such as the IC + MG oligomers shown in Scheme 1, could potentially undergo fragmentation in the ion source to produce the protonated IC, giving rise to additional smaller peaks in the  $m/z$  125.0709 SIC at longer retention times shown in Figure S3.

Lin et al. carried out analyses of a similar MG/AS BrC system in which bulk aqueous solutions containing MG and AS were aged over several days.<sup>17</sup> Figure S4 compares the PDA chromatogram from that work with the one recorded in this study. The slow aging method used by Lin et al. produced 30 chromophores with assignable formulas,<sup>17</sup> as opposed to the evaporation method used in this study that produced BrC within minutes but only resulted in one dominant absorbing species, specifically IC. Another difference is that Lin et al. had higher concentrations of MG and AS and desalted the sample before the analysis.<sup>17</sup> In our work here, the concentrations were

lower and no desalting was done. The dramatic difference in the resulting chromatograms of these two MG/AS systems indicates that various pathways of atmospheric aging may have significant effects on the molecular structures of BrC chromophores.

The IC peak at 12 min greatly decreased in intensity upon exposure to UV irradiation, as shown in Figure 6b. Exposure to radiation can cause the IC to undergo different photochemical reactions. One example is a Norrish type I reaction causing cleavage at the carbonyl carbon and leading to two free radical fragments that can then undergo secondary processes to form a variety of products.<sup>30</sup> Norrish type I photolysis processes generally have high photolysis quantum yields, in agreement with the large observed effective QY values reported in Table 1. The irradiation can also generate an electronically excited IC, which can react with a hydrogen donor (such as another IC, alcohols, or aldehydes) to form an aromatic alkoxy radical, also leading to a different set of products.<sup>30</sup>

NaBH<sub>4</sub> is expected to reduce IC to the corresponding alcohol (neutral formula C<sub>6</sub>H<sub>10</sub>ON<sub>2</sub>, protonated ion  $m/z$  127.0866) as shown in Scheme 2. An abundant ion with this  $m/z$  generated two peaks around 8 min in the NaBH<sub>4</sub> reduction sample. Figure 6c also shows a coeluting chromophoric species at 8 min with an absorption peak at 320 nm. Based on the structure of the reduced IC, we do not expect it to have any absorption bands at 320 nm. Thus, the 8 min peak in the PDA chromatogram must be from another coeluting compound (which we could not identify). We also found that methyl imidazole (C<sub>4</sub>H<sub>6</sub>N<sub>2</sub>) was a major new species in the NaBH<sub>4</sub> reduction sample. Methyl imidazole does not absorb in the near-UV and therefore does not show up in the PDA chromatogram in Figure 6, but it does absorb strongly at 220 nm and results in a large peak eluting near this wavelength at 7.5 min. Dimethyl imidazole was also detected in the NaBH<sub>4</sub> reduction sample, presumably resulting from the IC2 isomer (Scheme 2). These results indicate that the action of NaBH<sub>4</sub> is not simply a reduction of the carbonyl groups and that the addition of NaBH<sub>4</sub> to the MG/AS BrC solution initiates more complex processes that cleave C–C bonds.

A few other major ions were detected in the initial MG/AS BrC sample that did not correlate to any of the PDA peaks of the BrC chromophores. For example, there was a prominent group of peaks that eluted at a variety of retention times in both the dark control and photolysis samples. The  $m/z$  values of these species and corresponding neutral formulas were 306.1183 (C<sub>12</sub>H<sub>19</sub>NO<sub>8</sub>), 324.1289 (C<sub>12</sub>H<sub>21</sub>NO<sub>9</sub>), and 342.1395 (C<sub>12</sub>H<sub>23</sub>NO<sub>10</sub>). Each of these species is produced by combining four MG units and one NH<sub>3</sub>, with added hydration and dehydration steps. Other observed species that follow a similar formation pattern occurred at  $m/z$  252.1078 (C<sub>9</sub>H<sub>17</sub>NO<sub>7</sub>) and 234.0972 (C<sub>9</sub>H<sub>15</sub>NO<sub>6</sub>), both comprising three MG units. Scheme S2 in the Supporting Information illustrates plausible formation mechanisms of these compounds. However, whereas these open-chain compounds are prominent in the mixture, they are not sufficiently conjugated to absorb in the near-UV and visible range.

#### 4. SUMMARY

The products of the G + AS and MG + AS reactions and aged LIM/O<sub>3</sub> SOA attracted much attention as model BrC systems.<sup>2</sup> Our results, as well as previous experiments on the photochemistry of MG/AS system,<sup>12,15</sup> suggest that MG/AS BrC has a low photochemical stability. For example, with the QY from

Table 1 and the measured MAC from Figure 1, we estimate a photolysis lifetime for MG/AS BrC of about 13 min at zero solar zenith angle at sea level. This estimated lifetime is comparable to that determined by Sareen et al.<sup>12</sup> and Zhao et al.<sup>15</sup> The lifetime for the photobleaching of the aged LIM/O<sub>3</sub> SOA is also relatively short, on the order of 1 h.<sup>22</sup> Whereas the lifetimes will increase somewhat under cloudy conditions and at lower solar zenith angles, the potential impact of these photolabile BrC species on climate may be limited. Even if a sufficient amount of BrC were produced during the night, it would be readily photobleached upon sunrise and make minor contribution to the absorption of solar radiation for the rest of the day.

Another implication of this work is that the results of NaBH<sub>4</sub> addition to BrC or any other environmental mixture for the purpose of selective reduction of carbonyl groups to hydroxyl groups should be interpreted with care. This reaction is routinely used as a test for the presence of CT complexes in atmospheric BrC.<sup>18,31</sup> However, in the MG/AS BrC system, the addition of a small amount of NaBH<sub>4</sub> had complex effects on the absorption and fluorescence spectra. The excess amount of NaBH<sub>4</sub> did remove the major UV absorber, the imidazole carbonyl, as expected. However, the imidazole carbonyl is a small molecule that does not require intermolecular CT to absorb radiation. Furthermore, NaBH<sub>4</sub> appeared to lead to additional reactions other than simple reduction of carbonyl groups, which broke C–C bonds in the compounds. We can conclude that the reduction by NaBH<sub>4</sub> can lead to a decrease in the absorption of the mixture, but it has little to do with the removal of CT complexes. Recent results relying on HPLC-PDA-HRMS data show that, at least in some BrC systems, including MG/AS BrC, the overall absorption of the mixture is dominated by spectra of isolated chromophores and not CT complexes.<sup>17,32</sup>

The last conclusion of this work is that processes accelerated by evaporation of water can produce very different results compared to slow reactions in aqueous solution. We previously showed that evaporation of water from a solution of limonene ozonolysis SOA and ammonium sulfate accelerated BrC formation by a large factor.<sup>20</sup> This work, as well as work by Zhao et al.,<sup>15</sup> showed that evaporation not only accelerated BrC formation in the MG/AS system but also resulted in a completely different distribution of the chromophores. The evaporation conditions used in this work (bulk solution evaporated for ~20 min at 30 °C) may not fully replicate the much faster evaporation of water from cloud and fog droplets or from aerosol particles containing liquid water. However, the available data strongly suggest that the evaporative pathway for producing BrC should be relevant to the atmospheric environment because of the frequent changes in relative humidity and high frequency of fog and cloud droplet formation followed by evaporation. We recommend that future studies of secondary BrC formation in water should always include an evaporation test to check if BrC formation is enhanced (with the experiments ideally carried out with aerosolized droplets instead of a bulk solution).

## ■ ASSOCIATED CONTENT

### 📄 Supporting Information

The Supporting Information is available free of charge on the ACS Publications website at DOI: 10.1021/acsearthspacechem.7b00075.

Photolysis quantum yield calculations, most abundant peaks observed in high-resolution mass spectra, possible structures of oligomeric compounds, double bond equivalents and elemental composition of the observed compounds, and HPLC-PDA-HRMS data (PDF)

## ■ AUTHOR INFORMATION

### Corresponding Author

\*Phone: 949-824-1262. E-mail: nizkorod@uci.edu.

### ORCID

Alexander Laskin: 0000-0002-7836-8417

Julia Laskin: 0000-0002-4533-9644

Sergey A. Nizkorodov: 0000-0003-0891-0052

### Notes

The authors declare no competing financial interest.

## ■ ACKNOWLEDGMENTS

The authors acknowledge support by the U.S. Department of Commerce, National Oceanic and Atmospheric Administration through Climate Program Office's AC4 program, awards NA16OAR4310101 and NA16OAR4310102. P.A. thanks the Ford Foundation Predoctoral Fellowship Program of the National Academy of Science and the National Science Foundation Graduate Research Fellowship Program for their support. EEM measurements were performed at the Laser Spectroscopy Facility at UCI. The HR-ESI-MS measurements were performed at the W.R. Wiley Environmental Molecular Sciences Laboratory (EMSL)—a national scientific user facility located at PNNL, and sponsored by the Office of Biological and Environmental Research of the U.S. PNNL is operated for U.S. DOE by Battelle Memorial Institute under Contract No. DE-AC06-76RLO 1830.

## ■ REFERENCES

- (1) Fu, T. M.; Jacob, D. J.; Wittrock, F.; Burrows, J. P.; Vrekoussis, M.; Henze, D. K. Global budgets of atmospheric glyoxal and methylglyoxal, and implications for formation of secondary organic aerosols. *J. Geophys. Res.* **2008**, *113*, D15303.
- (2) Laskin, A.; Laskin, J.; Nizkorodov, S. A. Chemistry of atmospheric brown carbon. *Chem. Rev.* **2015**, *115* (10), 4335–4382.
- (3) Grimmett, M. R.; Richards, E. L. 686. Imidazole compounds from the reaction of pyruvaldehyde with ammonia. *J. Chem. Soc.* **1965**, 3751–3754.
- (4) Freedman, M. A.; Hasenkopf, C. A.; Beaver, M. R.; Tolbert, M. A. Optical properties of internally mixed aerosol particles composed of dicarboxylic acids and ammonium sulfate. *J. Phys. Chem. A* **2009**, *113* (48), 13584–13592.
- (5) Hawkins, L. N.; Baril, M. J.; Sedehi, N.; Galloway, M. M.; De Haan, D. O.; Schill, G. P.; Tolbert, M. A. Formation of semisolid, oligomerized aqueous SOA: lab simulations of cloud processing. *Environ. Sci. Technol.* **2014**, *48* (4), 2273–2280.
- (6) De Haan, D. O.; Corrigan, A. L.; Tolbert, M. A.; Jimenez, J. L.; Wood, S. E.; Turley, J. J. Secondary organic aerosol formation by self-reactions of methylglyoxal and glyoxal in evaporating droplets. *Environ. Sci. Technol.* **2009**, *43* (21), 8184–8190.
- (7) De Haan, D. O.; Hawkins, L. N.; Kononenko, J. A.; Turley, J. J.; Corrigan, A. L.; Tolbert, M. A.; Jimenez, J. L. Formation of nitrogen-containing oligomers by methylglyoxal and amines in simulated evaporating cloud droplets. *Environ. Sci. Technol.* **2011**, *45* (3), 984–991.
- (8) Sareen, N.; Schwier, A. N.; Shapiro, E. L.; Mitroo, D.; McNeill, V. F. Secondary organic material formed by methylglyoxal in aqueous aerosol mimics. *Atmos. Chem. Phys.* **2010**, *10* (3), 997–1016.

- (9) Maxut, A.; Noziere, B.; Fenet, B.; Mechakra, H. Formation mechanisms and yields of small imidazoles from reactions of glyoxal with  $\text{NH}_4^+$  in water at neutral pH. *Phys. Chem. Chem. Phys.* **2015**, *17* (31), 20416–20424.
- (10) Kampf, C. J.; Filippi, A.; Zuth, C.; Hoffmann, T.; Opatz, T. Secondary brown carbon formation via the dicarbonyl imine pathway: nitrogen heterocycle formation and synergistic effects. *Phys. Chem. Chem. Phys.* **2016**, *18* (27), 18353–18364.
- (11) Kampf, C. J.; Jakob, R.; Hoffmann, T. Identification and characterization of aging products in the glyoxal/ammonium sulfate system-implications for light-absorbing material in atmospheric aerosols. *Atmos. Chem. Phys.* **2012**, *12* (14), 6323–6333.
- (12) Sareen, N.; Moussa, S. G.; McNeill, V. F. Photochemical aging of light-absorbing secondary organic aerosol material. *J. Phys. Chem. A* **2013**, *117* (14), 2987–2996.
- (13) Woo, J. L.; Kim, D. D.; Schwiier, A. N.; Li, R.; McNeill, V. F. Aqueous aerosol SOA formation: impact on aerosol physical properties. *Faraday Discuss.* **2013**, *165*, 357–367.
- (14) McNeill, V. F.; Woo, J. L.; Kim, D. D.; Schwiier, A. N.; Wannell, N. J.; Sumner, A. J.; Barakat, J. M. Aqueous-phase secondary organic aerosol and organosulfate formation in atmospheric aerosols: a modeling study. *Environ. Sci. Technol.* **2012**, *46* (15), 8075–8081.
- (15) Zhao, R.; Lee, A. K.; Abbatt, J. P. D. Investigation of aqueous-phase photooxidation of glyoxal and methylglyoxal by aerosol chemical ionization mass spectrometry: observation of hydroxyhydroperoxide formation. *J. Phys. Chem. A* **2012**, *116* (24), 6253–6263.
- (16) Lee, A. K.; Zhao, R.; Li, R.; Liggio, J.; Li, S. M.; Abbatt, J. P. Formation of light absorbing organo-nitrogen species from evaporation of droplets containing glyoxal and ammonium sulfate. *Environ. Sci. Technol.* **2013**, *47* (22), 12819–12826.
- (17) Lin, P.; Laskin, J.; Nizkorodov, S. A.; Laskin, A. Revealing brown carbon chromophores produced in reactions of methylglyoxal with ammonium sulfate. *Environ. Sci. Technol.* **2015**, *49* (24), 14257–14266.
- (18) Phillips, S. M.; Smith, G. D. Light absorption by charge transfer complexes in brown carbon aerosols. *Environ. Sci. Technol. Lett.* **2014**, *1* (10), 382–386.
- (19) Sharpless, C. M.; Blough, N. V. The importance of charge-transfer interactions in determining chromophoric dissolved organic matter (CDOM) optical and photochemical properties. *Environ. Sci. Processes & Impacts* **2014**, *16* (4), 654–671.
- (20) Nguyen, T. B.; Lee, P. B.; Updyke, K. M.; Bones, D. L.; Laskin, J.; Laskin, A.; Nizkorodov, S. A. Formation of nitrogen- and sulfur-containing light-absorbing compounds accelerated by evaporation of water from secondary organic aerosols. *J. Geophys. Res.* **2012**, *117*, D01207.
- (21) Epstein, S. A.; Shemesh, D.; Tran, V. T.; Nizkorodov, S. A.; Gerber, R. B. Absorption spectra and photolysis of methyl peroxide in liquid and frozen water. *J. Phys. Chem. A* **2012**, *116* (24), 6068–6077.
- (22) Lee, H. J.; Aiona, P. K.; Laskin, A.; Laskin, J.; Nizkorodov, S. A. Effect of solar radiation on the optical properties and molecular composition of laboratory proxies of atmospheric brown carbon. *Environ. Sci. Technol.* **2014**, *48* (17), 10217–10226.
- (23) Bunce, N. J.; LaMarre, J.; Vaish, A. P. Photorearrangement of azoxybenzene to 2-hydroxyazobenzene: a convenient chemical actinometer. *Photochem. Photobiol.* **1984**, *39* (4), 531–533.
- (24) Nguyen, T. K. V.; Zhang, Q.; Jimenez, J. L.; Pike, M.; Carlton, A. G. Liquid water: ubiquitous contributor to aerosol mass. *Environ. Sci. Technol. Lett.* **2016**, *3* (7), 257–263.
- (25) Chen, Y.; Bond, T. C. Light absorption by organic carbon from wood combustion. *Atmos. Chem. Phys.* **2010**, *10* (4), 1773–1787.
- (26) Powelson, M. H.; Espelien, B. M.; Hawkins, L. N.; Galloway, M. M.; De Haan, D. O. Brown carbon formation by aqueous-phase carbonyl compound reactions with amines and ammonium sulfate. *Environ. Sci. Technol.* **2014**, *48* (2), 985–993.
- (27) Hawkins, L. N.; Lemire, A. N.; Galloway, M. M.; Corrigan, A. L.; Turley, J. J.; Espelien, B. M.; De Haan, D. O. Maillard chemistry in clouds and aqueous aerosol as a source of atmospheric humic-like substances. *Environ. Sci. Technol.* **2016**, *50* (14), 7443–7452.
- (28) Romonosky, D. E.; Laskin, A.; Laskin, J.; Nizkorodov, S. A. High-resolution mass spectrometry and molecular characterization of aqueous photochemistry products of common types of secondary organic aerosols. *J. Phys. Chem. A* **2015**, *119* (11), 2594–2606.
- (29) Epstein, S. A.; Blair, S. L.; Nizkorodov, S. A. Direct photolysis of alpha-pinene ozonolysis secondary organic aerosol: effect on particle mass and peroxide content. *Environ. Sci. Technol.* **2014**, *48* (19), 11251–11258.
- (30) George, C.; Ammann, M.; D'Anna, B.; Donaldson, D. J.; Nizkorodov, S. A. Heterogeneous photochemistry in the atmosphere. *Chem. Rev.* **2015**, *115* (10), 4218–4258.
- (31) Phillips, S. M.; Smith, G. D. Further evidence for charge transfer complexes in brown carbon aerosols from excitation-emission matrix fluorescence spectroscopy. *J. Phys. Chem. A* **2015**, *119* (19), 4545–4551.
- (32) Lin, P.; Aiona, P. K.; Li, Y.; Shiraiwa, M.; Laskin, J.; Nizkorodov, S. A.; Laskin, A. Molecular characterization of brown carbon in biomass burning aerosol particles. *Environ. Sci. Technol.* **2016**, *50* (21), 11815–11824.